

Chemistry–A European Journal

Supporting Information

A Nonaqueous Redox-Matched Flow Battery with Charge Storage in Insoluble Polymer Beads

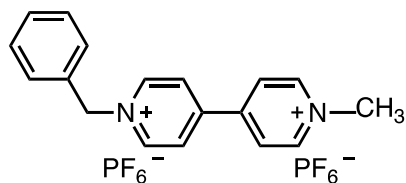
Dukhan Kim, Melanie S. Sanford, Thomas P. Vaid,* and Anne J. McNeil*

Table of Contents

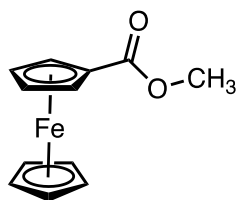
I.	Structures and Abbreviations.....	2
II.	Materials.....	3
III.	Materials Characterization	3
IV.	Synthetic Procedures	4
V.	NMR Spectra.....	7
VI.	IR and Raman Spectra	11
VII.	Swelling Measurements	12
VIII.	Electrochemical Materials and Methods	13
IX.	Materials Preparation via Bulk Electrolysis	15
X.	Cyclic Voltammograms of Electrolyte over Beads vs Mediators Solution	16
XI.	Bead-Mediator Redox Exchange Rate in Reservoir with Flow	17
XII.	Screening Crossover Rates with Various Membranes	18
XIII.	Flow Cell Cycling with Celgard Membrane or with xPS-Cl Beads	22
XIV.	References.....	23

I. Structures and Abbreviations

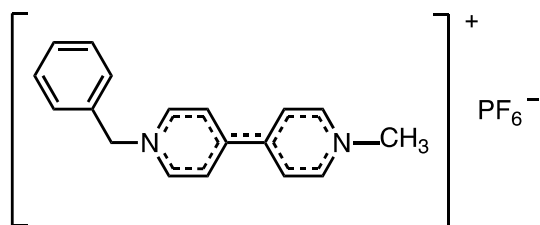
Soluble Mediators



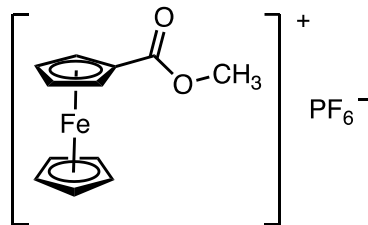
[Bn-bpy-Me²⁺][PF₆⁻]₂



FcR

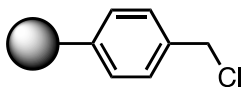


[Bn-bpy-Me⁺][PF₆⁻]

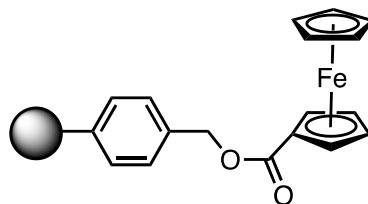


[FcR⁺][PF₆⁻]

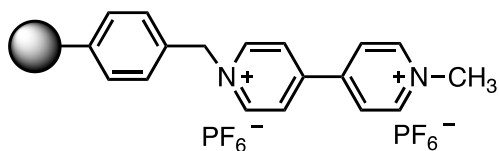
Insoluble beads



xPS-Cl



xPS-FcR



[xPS-bpy-Me²⁺][PF₆⁻]₂

II. Materials

4,4'-Dipyridyl, iodomethane, benzyl bromide, ammonium hexafluorophosphate (NH_4PF_6), ferrocene carboxylic acid, diisopropylethylamine, and silver hexafluorophosphate were purchased from Sigma Aldrich and used without further purification. Methyl ferrocenecarboxylate (**FcR**) was purchased from Ambeed and used after sublimation. Merrifield resin (poly(chloromethylstyrene-co-styrene-co-divinylbenzene) (200–400 mesh, 3.5–4.5 mmol/g Cl, 1% cross-linked) (**xPS-Cl**) was purchased from Sigma Aldrich. Dichloromethane (DCM), ethyl acetate (EtOAc), methanol (MeOH), acetonitrile (MeCN), dimethylformamide (DMF), and diethyl ether (Et_2O) were purchased from Sigma Aldrich or Fisher and used without purification.

III. Materials Characterization

NMR Spectroscopy – ^1H and ^{13}C NMR spectra for all compounds were acquired at rt. Chemical shift data are reported in units of δ (ppm) relative to tetramethylsilane (TMS) and referenced with residual solvent. Multiplicities are reported as follows: singlet (s), doublet (d), doublet of doublets (dd), triplet (t), quartet (q), multiplet (m).

Element Analysis (EA) – EA was performed by Midwest Microlab. EA for **xPS-Cl** was C: 78.27%, H: 6.66%, Cl: 14.87%, indicating that 1 g of **xPS-Cl** has 4.2 mmol of Cl. This number was used for further measurements of functionalized beads.

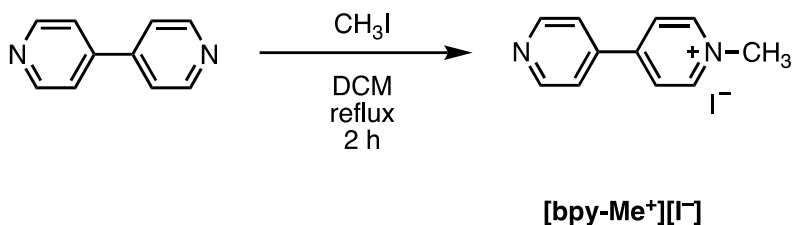
Infrared Spectroscopy (IR) – IR data were recorded using a Thermo Scientific Nicolet IS50 FT-IR spectrometer.

Raman Spectroscopy – Raman data were recorded using a Renishaw inVia Raman microscope equipped with a RenCam CCD detector, a 785 nm diode laser, 1200 lines/mm grating, and a 65 μm slit. Spectra were analyzed using the WiRE 3.4 software package and calibrated using a silicon standard.

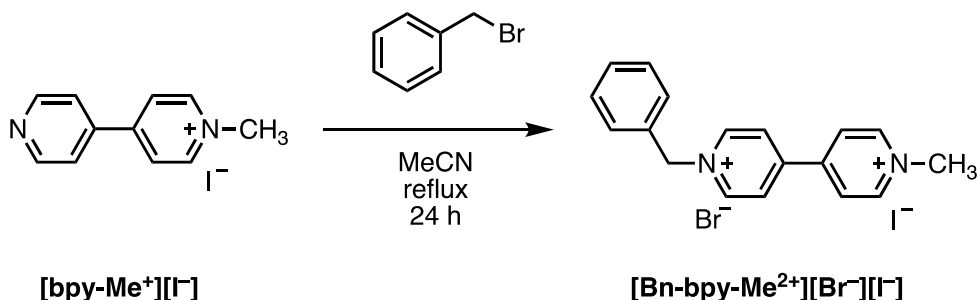
Swelling Measurement – Optical Microscopy – Before measurements, the beads were dried under vacuum. The crosslinked polymer beads were soaked in MeCN or DMF for 60 min then examined while still in the solvent, using a microscope slide and a cover slip to contain the solvent, using a Leica DMCB optical microscope with a 10x objective lens. Images were recorded with an attached QICAM Fast 1394 digital video camera. Similar images of pristine beads were collected. The average diameter was calculated by ImageJ from over 300 beads before and after soaking.

Swelling Measurement – Volumetric Change – In an NMR tube, a precisely measured mass (~100 mg) of polymer beads was added, and the height was measured and used for calculating the volume change upon swelling using conversion factor 1 cm height = 130 μL . The height of the beads was recorded before and after soaking in MeCN or DMF for 60 min.

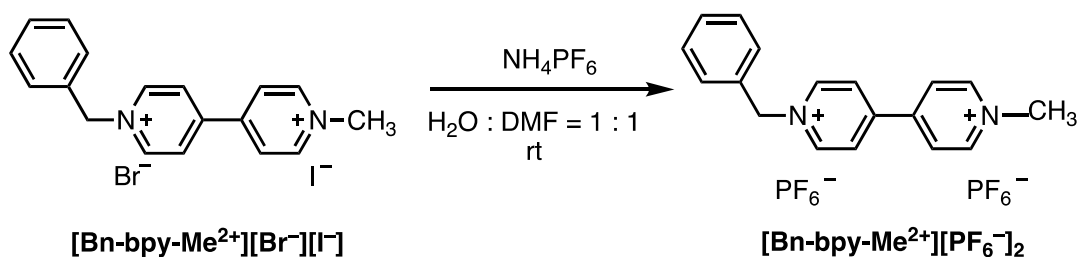
IV. Synthetic Procedures



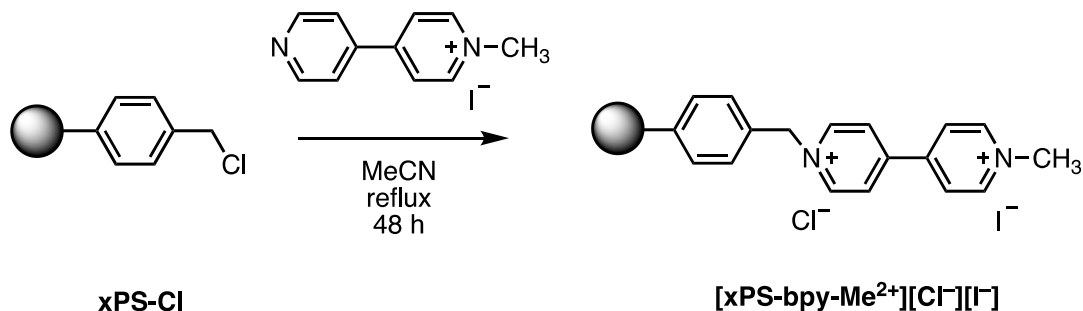
[bpy-Me⁺][I⁻]. (This is a slight modification of a reported procedure.¹) In an oven-dried 100 mL round-bottom flask, a mixture of 4,4'-dipyridyl (784 mg, 5.02 mmol) and iodomethane (0.41 mL, 6.6 mmol, 1.3 equiv.) in DCM (10 mL) was stirred at reflux under N₂ for 2 h, during which time a yellow precipitate formed. After cooling to rt, the yellow precipitate was collected and washed with EtOAc (2 x 50 mL) and Et₂O (2 x 50 mL). The solid was recrystallized from MeOH to yield **[bpy-Me⁺][I⁻]** as a yellow powder (1.13 g, 75% yield). ¹H NMR (401 MHz, DMSO-d₆) δ 9.15 (d, *J* = 6.5 Hz, 2H), 8.91 – 8.82 (m, 2H), 8.67 – 8.58 (m, 2H), 8.08 – 8.00 (m, 2H), 4.39 (s, 3H). ¹³C NMR (126 MHz, DMSO-d₆) δ 152.29, 151.48, 146.61, 141.29, 125.40, 122.32, 48.05.



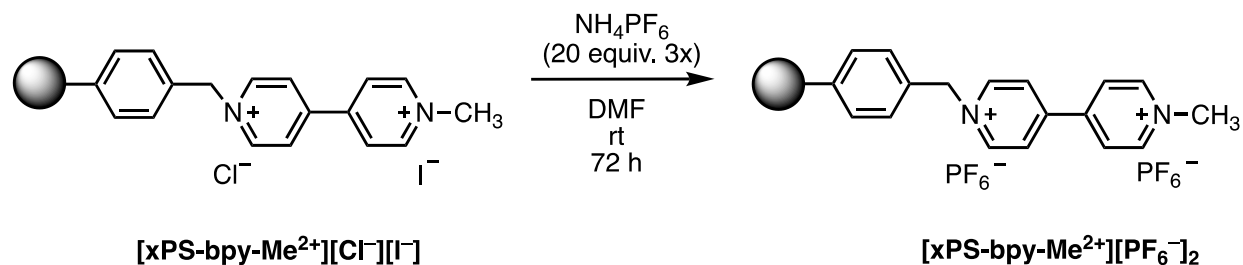
[Bn-bpy-Me²⁺][Br⁻][I⁻]. (This is a modified version of a reported procedure.²) In a 100 mL round-bottom flask, a mixture of **[bpy-Me⁺][I⁻]** (415.7 mg, 1.395 mmol) and benzyl bromide (285 mg, 1.67 mmol, 1.2 equiv.) in MeCN (20.0 mL) was stirred at reflux for 24 h, during which time a red precipitate formed. After cooling to rt, the red precipitate was collected and washed with EtOAc (2 x 100 mL). The red powder was collected to yield **[Bn-bpy-Me²⁺][Br⁻][I⁻]** (561 mg, 86% yield). ¹H NMR (401 MHz, DMSO-d₆) δ 9.60 (d, *J* = 6.7 Hz, 2H), 9.33 (d, *J* = 6.6 Hz, 2H), 8.90 – 8.72 (m, 4H), 7.72 – 7.60 (m, 2H), 7.52 – 7.40 (m, 3H), 6.01 (s, 2H), 4.46 (s, 3H). ¹³C NMR (126 MHz, DMSO) δ 149.54, 148.60, 147.04, 146.19, 134.70, 129.97, 129.73, 129.49, 127.55, 126.67, 63.65, 48.49.



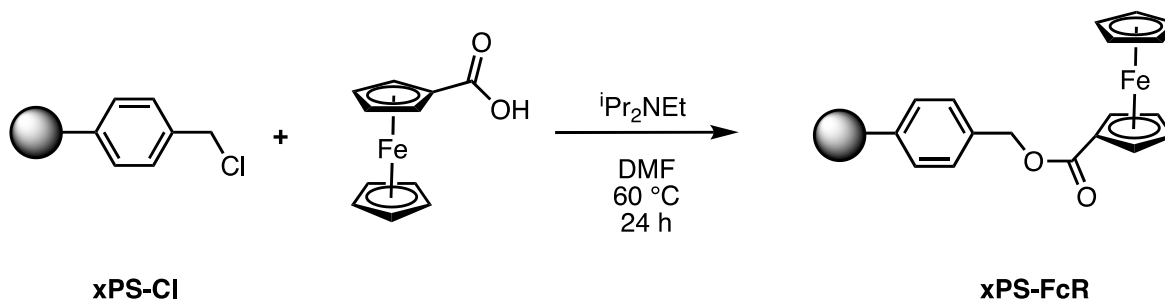
[Bn-bpy-Me²⁺][PF₆⁻]₂. In a 20 mL vial, **[Bn-bpy-Me²⁺][Br⁻][I⁻]** (100 mg, 0.214 mmol) was dissolved in a 1:1 mixture of deionized water (2.5 mL) and DMF (2.5 mL). This homogenous solution was added dropwise via syringe into another 20 mL vial containing excess NH₄PF₆ (192 mg, 1.18 mmol, 5.5 equiv.) in water (10 mL). A yellow precipitate formed instantly. The yellow solid was collected by filtration and then washed with water (2 x 50 mL). The solid was dried under vacuum to obtain **[Bn-bpy-Me²⁺][PF₆⁻]₂** as a yellow solid (118 mg, 97% yield). ¹H NMR (401 MHz, DMSO-d₆) δ 9.50 (d, *J* = 5.1 Hz, 2H), 9.26 (d, *J* = 6.6 Hz, 2H), 8.81 – 8.67 (m, 4H), 7.60 (d, *J* = 6.5 Hz, 2H), 7.47 (m, *J* = 7.8 Hz, 3H), 5.94 (s, *J* = 3.9 Hz, 2H), 4.51 – 4.36 (s, 3H). ¹³C NMR (126 MHz, DMSO) δ 149.67, 148.73, 147.02, 146.18, 134.58, 130.00, 129.76, 129.34, 127.54, 126.66, 63.95, 48.51.



[xPS-bpy-Me²⁺][Cl⁻][I⁻]. In a 100 mL round-bottom flask, a mixture of **[bpy-Me⁺][I⁻]** (197 mg, 0.66 mmol) and **xPS-Cl** (100 mg, 0.42 mmol Cl) in MeCN (30 mL) was heated to reflux for 48 h, during which time the beads turned red. After cooling to rt, the red beads were collected by filtration and then washed with MeCN (30 mL). The beads were transferred to a centrifuge tube using MeCN and soaked in MeCN (30 mL) for 30 min. The MeCN was decanted, then fresh MeCN was added (30 mL) and soaked for another 30 min. The MeCN was decanted. The red solid was dried and collected (75% conversion of the chloromethyl groups). (EA: C 65.48%, H 5.73%, N 2.51%, Cl 9.07%, I 13.77%) (theoretical EA for 75% conversion of the chloromethyl groups with 0.50 equiv of MeCN present: C 61.71%, H 5.36%, N 6.76%, Cl 7.10%, I 19.07%).



[xPS-bpy-Me²⁺][PF₆⁻]₂. In a 20 mL vial, **[xPS-bpy-Me²⁺][Cl⁻][I⁻]** (100 mg, 0.256 mmol Cl⁻, I⁻ each) and NH₄PF₆ (835 mg, 5.12 mmol, 20 equiv.) were added into DMF (15 mL) in a centrifuge tube. The mixture was agitated using a shaker (Sonics SHK-COCK2) for 24 h. Then, the supernatant was decanted, and NH₄PF₆ (835 mg, 5.12 mmol, 20 equiv.) in DMF (10 mL) solution was added. The mixture was shaken for another 24 h. The supernatant was decanted, and the procedure was repeated (for a total of three times). The beads were soaked for 30 min in neat DMF (50 mL) and the DMF then decanted. The beads were soaked for 30 min in neat MeCN (50 mL) and the MeCN then decanted. The yellow solid was vacuum dried and collected (95% ion exchange based on EA) (EA: C 57.37%, H 5.14%, N 3.44%, Cl 1.69%, I 0.93%, F 21.15%) (theoretical EA for 95% ion exchange and 75% conversion of chloromethyl groups in reaction above): C 51.78%, H 4.35%, N 3.80%, Cl 1.84%, I 0.86%, P 7.98%, F 29.38%).



xPS-FcR. In a 100 mL round-bottom flask, a mixture of **xPS-Cl** (200 mg, 0.840 mmol Cl), ferrocene carboxylic acid (242 mg, 1.05 mmol), and diisopropylethylamine (0.183 mL, 1.05 mmol) was stirred in DMF (30 mL) for 24 h at 60 °C. After cooling to rt, the dark brown beads were collected by filtration and washed with DMF (30 mL). Then the beads were transferred to a centrifuge tube using DMF and soaked in DMF (30 mL) for 30 min. The DMF was decanted, and fresh DMF (30 mL) was added and soaking repeated for another 30 min. The DMF was decanted, and MeCN (30 mL) was added soaking repeated for 30 min. The MeCN was decanted, and the MeCN wash was repeated for a total of 3 MeCN washes. The brown solid was vacuum dried and collected (70% conversion of the chloromethyl groups based on EA) (EA: C 72.26%, H 6.52%, N 1.05%, Cl 2.66%) (theoretical EA for 70% conversion of the chloromethyl groups with 0.16 equiv of DMF present: C 73.43%, H 6.10%, N 1.03%, Cl 2.69%, Fe 9.89%).

V. NMR Spectra

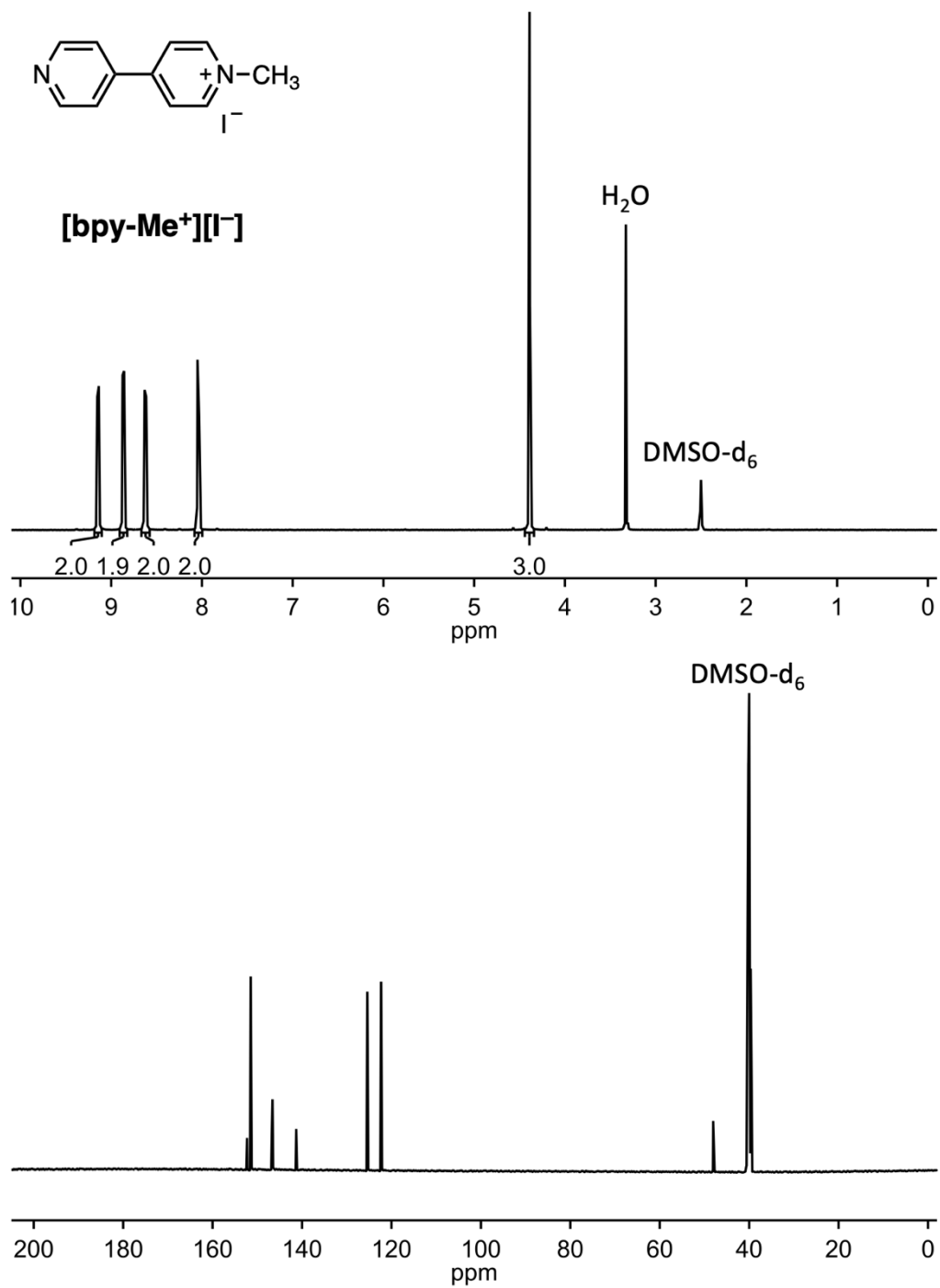


Figure S1. ¹H and ¹³C NMR Spectra of **[bpy-Me⁺][I⁻]**.

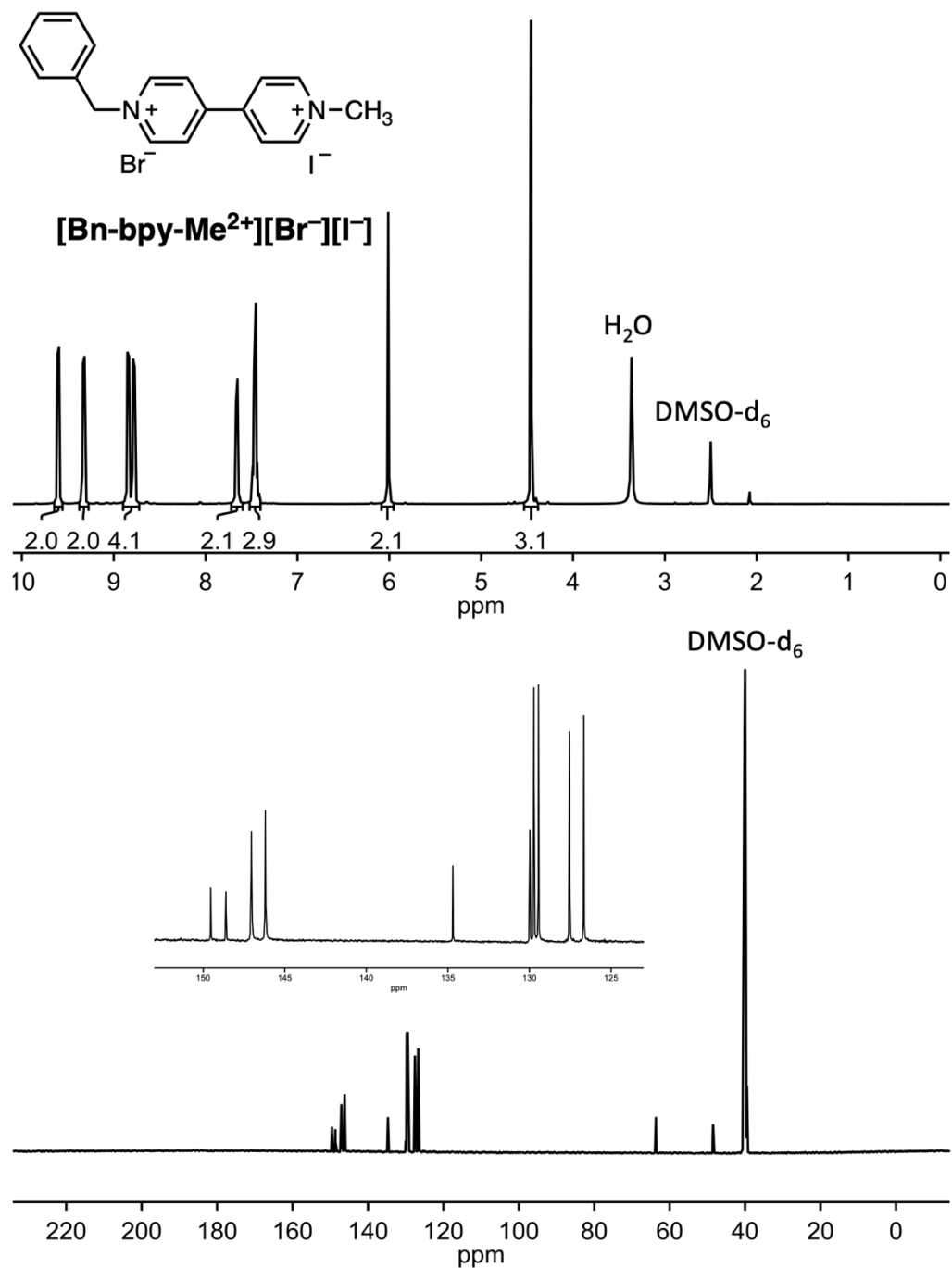


Figure S2. ^1H and ^{13}C NMR Spectra of $[\text{Bn-bpy-Me}^{2+}][\text{Br}^-][\text{I}^-]$.

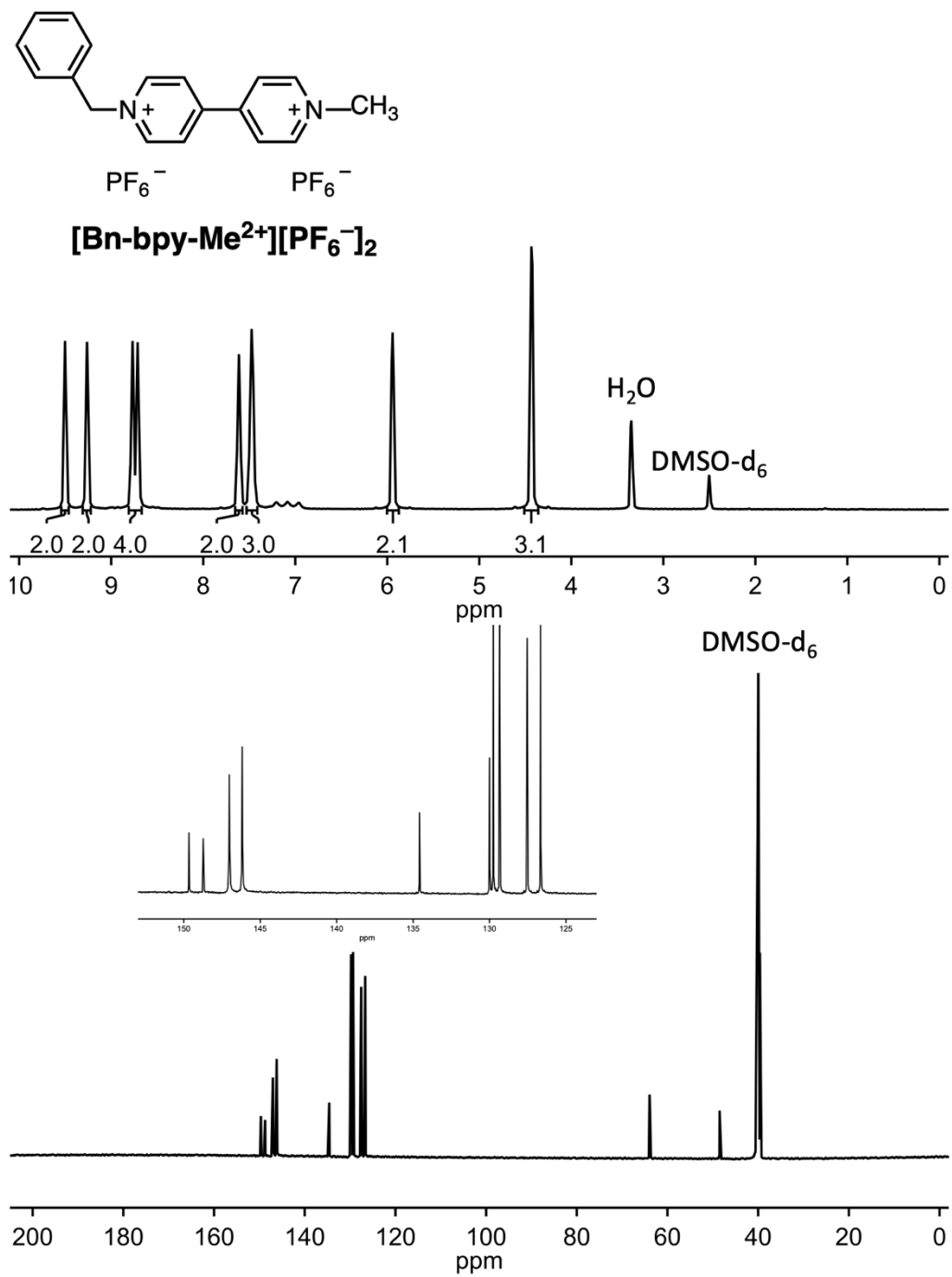


Figure S3. ¹H and ¹³C NMR Spectra of [Bn-bpy-Me²⁺][PF₆⁻]₂.

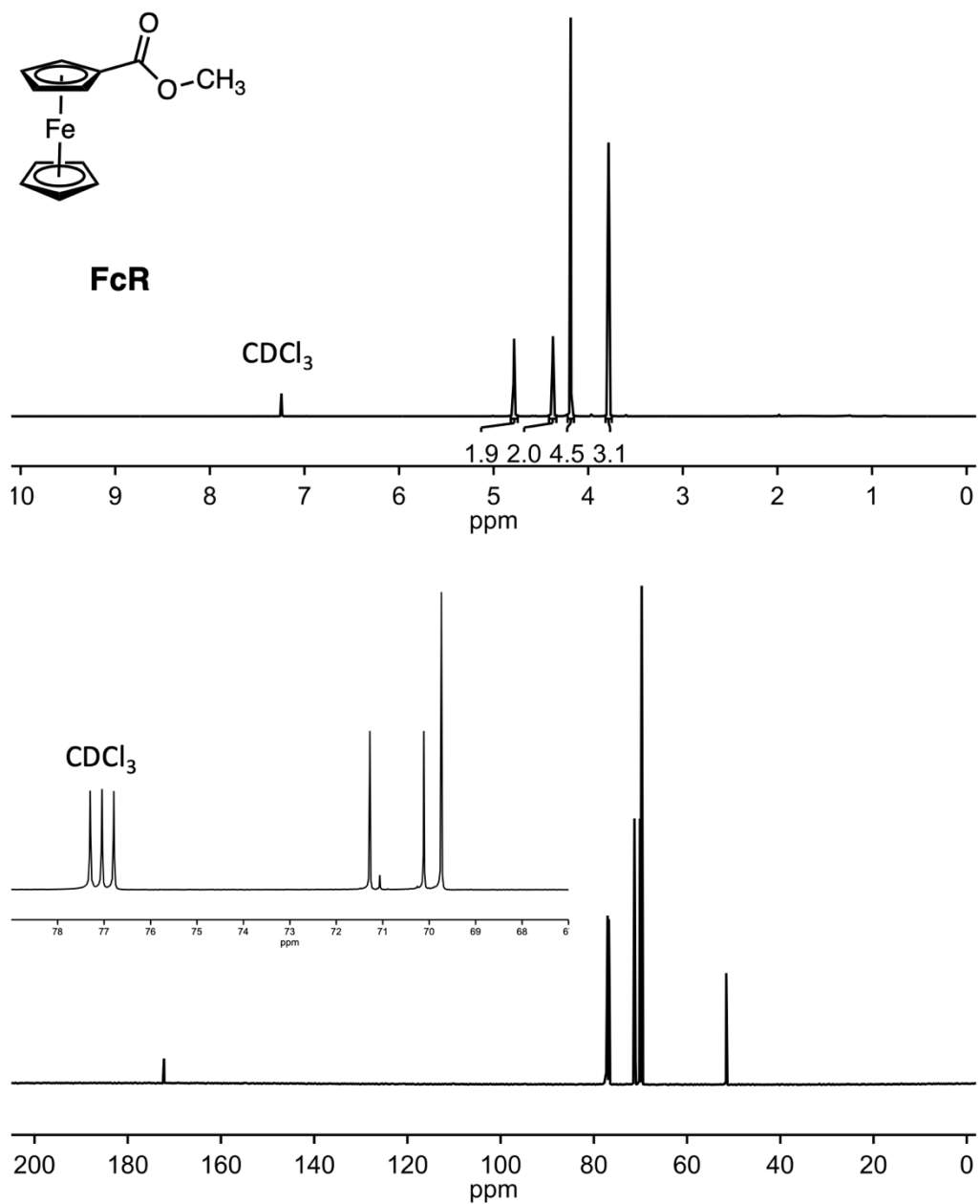


Figure S4. ^1H and ^{13}C NMR Spectra of **FcR**. ^1H NMR (401 MHz, CDCl_3) δ 4.78 (s, $J = 1.9$ Hz, 2H), 4.37 (s, $J = 2.0$ Hz, 2H), 4.19 (s, 5H), 3.79 (s, 3H). ^{13}C NMR (126 MHz, CDCl_3) δ 172.22, 71.28, 71.06, 70.25, 69.85, 51.60.

VI. IR and Raman Spectra

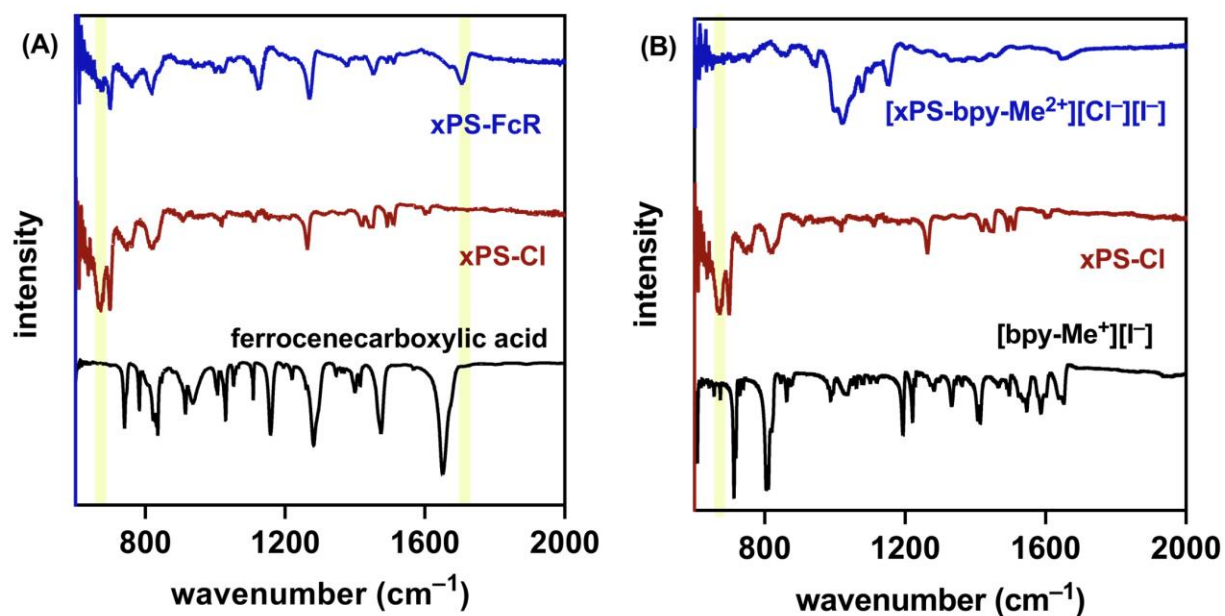


Figure S5. IR spectra of (A) **xPS-FcR**, **xPS-Cl** and ferrocene carboxylic acid, and (B) **[xPS-bpy-Me²⁺][Cl⁻][I⁻]**, **xPS-Cl**, and **[bpy-Me⁺][I⁻]**. C-Cl band at 672 cm⁻¹ and C=O band at 1714 cm⁻¹.

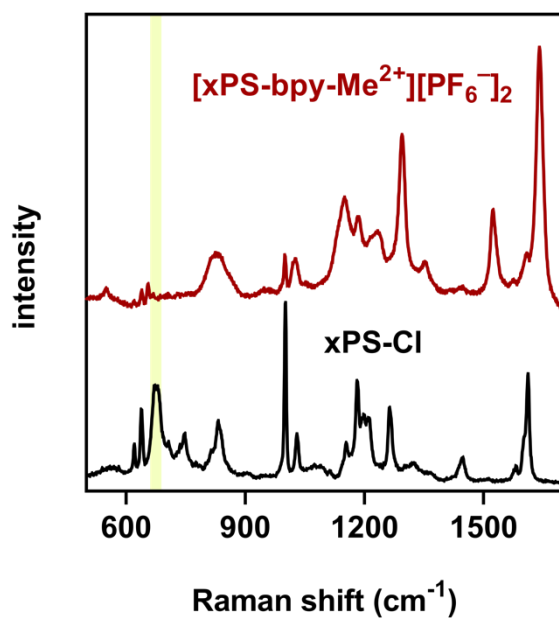


Figure S6. Raman spectra of **[xPS-bpy-Me²⁺][PF₆⁻]₂** and **xPS-Cl**. C-Cl band at 665 cm⁻¹.

VII. Swelling Measurements

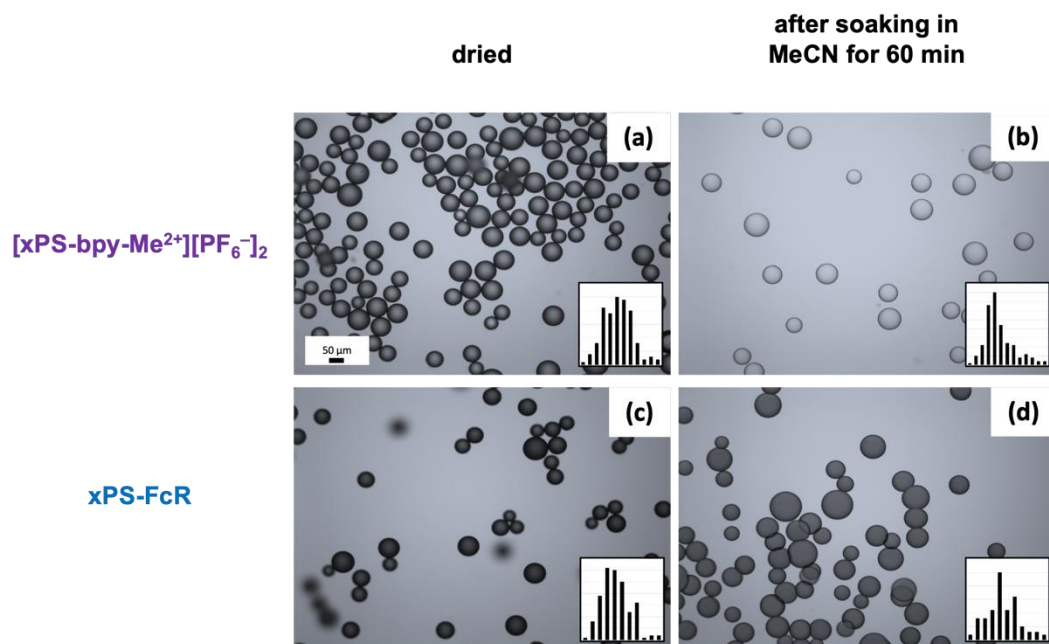


Figure S7. Optical microscope images of (a) dried [xPS-bpy-Me²⁺][PF₆⁻]₂ and (b) after soaking in MeCN for 60 min, (c) dried xPS-FcR and (d) after soaking in MeCN for 60 min. Each inset (bar charts) indicates the distribution of diameter of the beads.

Table S1. Swelling data of crosslinked beads.

method	calculated volume of each bead from radius measured by optical microscope			measured volume per 100 mg of each bead using NMR tube		
	dry	in MeCN	in DMF	dry	in MeCN	in DMF
xPS-Cl	52 pL	57 pL	194 pL	143 μL	169 μL	312 μL
xPS-FcR	81 pL	121 pL	269 pL	143 μL	247 μL	390 μL
[xPS-bpy-Me ²⁺][PF ₆ ⁻] ₂	82 pL	144 pL	211 pL	143 μL	273 μL	299 μL

VIII. Electrochemical Materials and Methods

General – Acetonitrile (MeCN) (99.8%, anhydrous) was obtained from Sigma Aldrich and used as received. Tetrabutylammonium hexafluorophosphate (TBAPF₆, electrochemical grade) and silver hexafluorophosphate (AgPF₆) were obtained from Sigma Aldrich and dried under high vacuum for 48 h before being transferred to a N₂-filled glovebox. A 0.50 M stock solution of the TBAPF₆ in MeCN was prepared in a N₂-filled glovebox (Mbraun Labmaster) with water < 4 ppm and oxygen < 0.5 ppm and dried over 3 Å molecular sieves for at least 2 days prior to use.

Cyclic Voltammetry – Cyclic voltammetry was performed in a N₂-filled glovebox with a Biologic VSP multichannel potentiostat/galvanostat and a three-electrode electrochemical cell, consisting of a glassy carbon disk working electrode (3.0 mm diameter, area 0.071 cm², BASi), an Ag/Ag⁺ reference electrode (BASi) with 0.010 M AgPF₆ in MeCN, and a platinum wire counter electrode (BASi). All experiments were conducted in a 0.50 M TBAPF₆/MeCN solution.

Ultramicroelectrode (UME) Experiments (Fig. S9–S13) – UME experiments were performed in a N₂-filled glovebox with a Biologic VSP multichannel potentiostat/galvanostat and a three-electrode electrochemical cell, consisting of an UME platinum disk working electrode (10 μm diameter, BASi), a silver wire quasi-reference electrode (BASi), and a platinum wire counter electrode (BASi). All experiments were conducted in a 0.50 M TBAPF₆/MeCN solution. Plateau currents in the CVs were used to calculate the concentrations of neutral and charged mediators.

Flow Cell Cycling (Fig. S14–S15)³ – Cycling under flow conditions was performed with a zero-gap flow cell comprised of graphite charge collecting plates containing an interdigitated flow field in combination with two layers of non-woven carbon felt electrodes (Sicracet 29AA) on each side. ePTFE gaskets were used to achieve ~20% compression of the felt. A membrane separated the two half cells, and the exposed area of the membrane in the gasket window was used as the active area (2.55 cm²). After assembly, both the catholyte side and anolyte side of the cell were loaded with a 15 mM (in each mediator) solution (12 mL) of 1:1 mixed **FcR:[Bn-bpy-Me²⁺][PF₆⁻]₂** in 0.50 M TBAPF₆/MeCN. The cell was pretreated by continuously flowing the solution above at 10 mL/min for 30 min without any charging process using a peristaltic pump (Cole-Parmer) with Solveflex and PFA tubing. After this step, using the same flow rate, galvanostatic charge/discharge cycling was performed using a BioLogic VSP galvanostat employing a charging current of 10 mA (3.92 mA/cm²) and a discharging current of -10 mA (-3.92 mA/cm²) with +1.6 V and +0.4 V voltage cut-off. After running the battery without beads, cycling and circulation were stopped. A targeted amount of **xPS-FcR** was added into catholyte reservoir and **[xPS-bpy-Me²⁺][PF₆⁻]₂** was added into anolyte reservoir. After this step, using the same flow rate, galvanostatic charge/discharge cycling was restarted.

Membranes

Celgard 2500 membranes were received from Asahi Kasei, Daramic 175 membranes were received from Daramic, LLC, and Fumasep (FAP-375-PP) ion-exchange membranes were received from Fuel Cell Store.

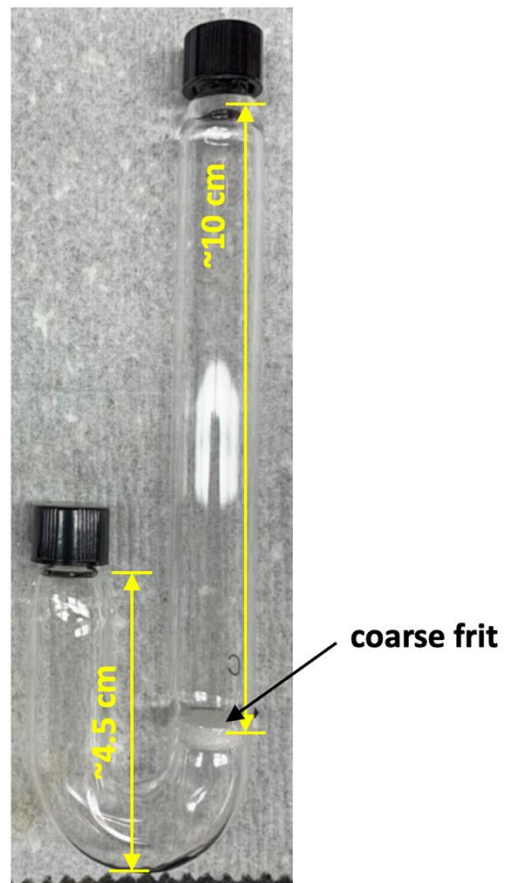
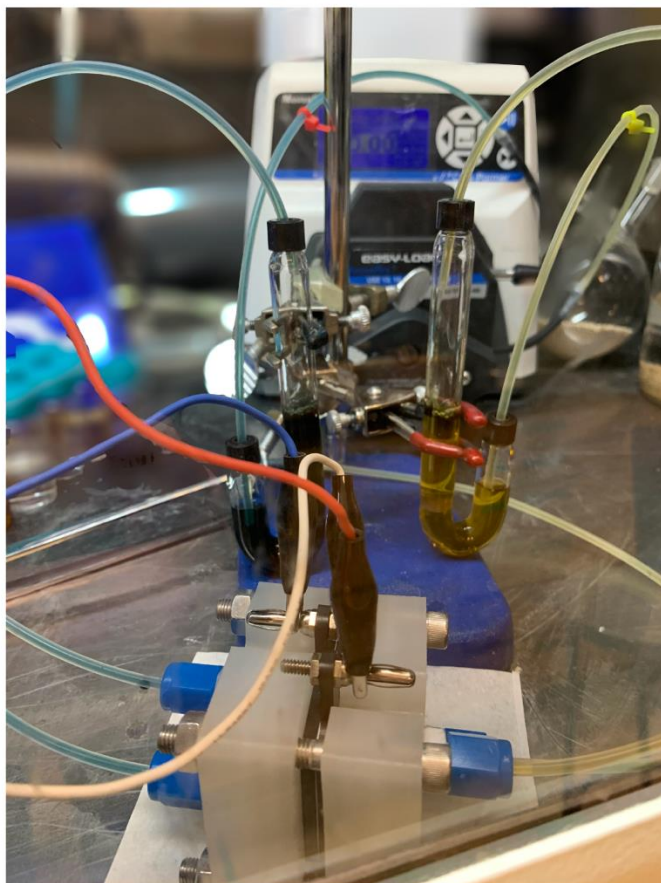
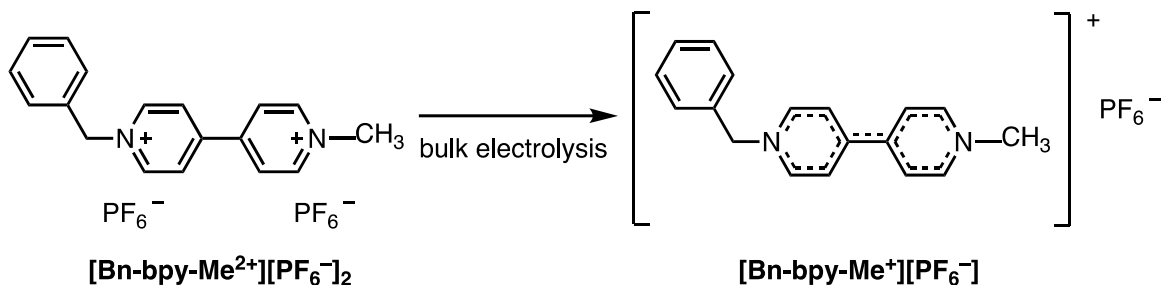
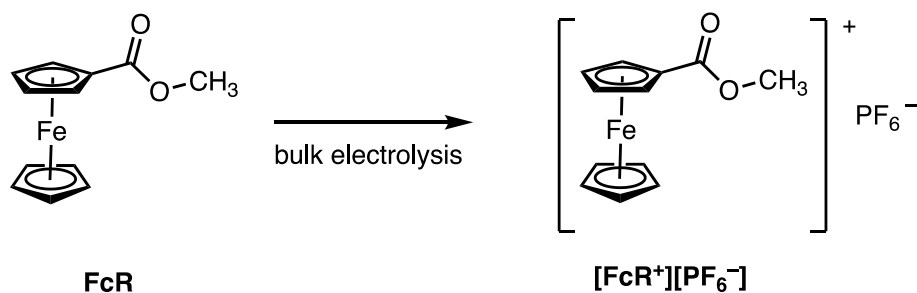


Figure S8. Redox-Matched Flow Battery setup with customized reservoirs

IX. Materials Preparation via Bulk Electrolysis



[Bn-bpy-Me⁺][PF₆⁻]. Bulk electrolysis was performed in an H-cell with an ultrafine fritted glass separator (P5, Adams and Chittenden). The experiments were performed in 0.50 M TBAPF₆ in MeCN with 5.0 mM of **[Bn-bpy-Me²⁺][PF₆⁻]₂**. The working and counter electrode were reticulated vitreous carbon 2" long (McMaster 100 PPI, ~0.25 inches diameter), and the reference electrode was Ag wire in 10 mM AgPF₆ + 0.50 M TBAPF₆ in MeCN in a glass tube separated by a 0.50 mm BASi CoralPore frit. The working chamber was charged against 5 mL of blank solution (0.50 M TBAPF₆ in MeCN), and the current was set to -5 mA under a predetermined voltaic cut-off of -1.5 V. When the potential reached the voltaic cut-off after 15 min XX seconds (X.XX mAh, XX% of theoretical), the charging was stopped and the solution in working side was collected.



[FcR⁺][PF₆⁻]. Bulk electrolysis as described above, except using a 5.0 mM solution of FcR and an oxidative current with a cutoff of +1.5 V.

X. Cyclic Voltammograms of Electrolyte over Beads vs Mediators Solution

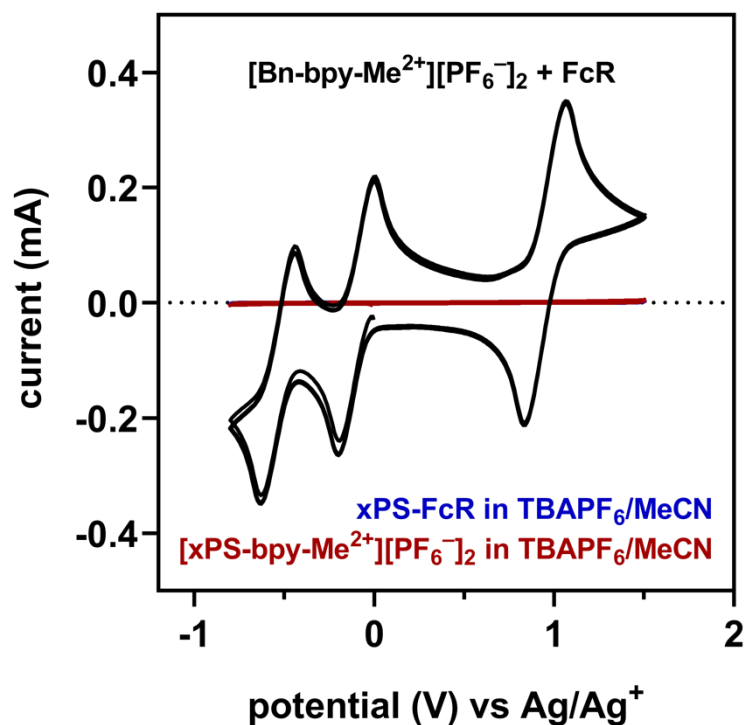


Figure S9. Cyclic voltammetry of 1:1 mixed solution of 5.0 mM **FcR** + 5.0 mM **[Bn-bpy-Me²⁺][PF₆⁻]₂** (black), **xPS-FcR** (blue, overlapped with red line), and **[xPS-bpy-Me²⁺][PF₆⁻]₂** (red) in 0.5 M TBAPF₆ in MeCN (showing no electroactive species are released from beads into a blank supporting electrolyte solution in MeCN).

XI. Bead-Mediator Redox Exchange Rate in Reservoir with Flow

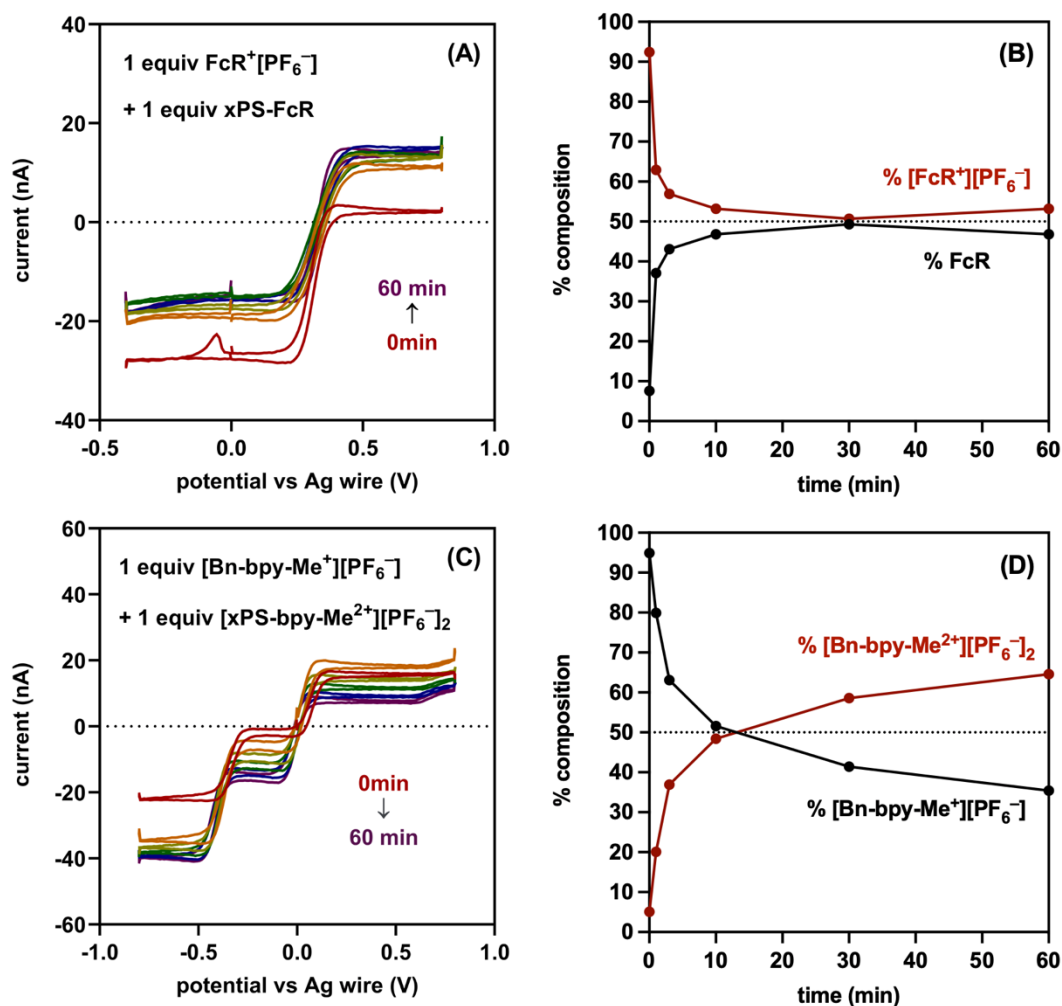


Figure S10. (A) Ultramicroelectrode cyclic voltammograms of $[\text{FcR}^+][\text{PF}_6^-]$ solution in contact with 1 equiv of xPS-FcR in the reservoir with recirculation by the pump (bypassing the cell stack). (B) Percentage of $[\text{FcR}^+][\text{PF}_6^-]$ and FcR present in solution over time. (C) Ultramicroelectrode cyclic voltammograms of $[\text{Bn-bpy-Me}^+][\text{PF}_6^-]$ solution in contact with 1 equiv of $[\text{xPS-bpy-Me}^{2+}][\text{PF}_6^-]_2$ in the reservoir with recirculation by the pump. (D) Percentage of $[\text{Bn-bpy-Me}^+][\text{PF}_6^-]$ and $[\text{Bn-bpy-Me}^{2+}][\text{PF}_6^-]_2$ present in solution over time.

XII. Screening Crossover Rates with Various Membranes

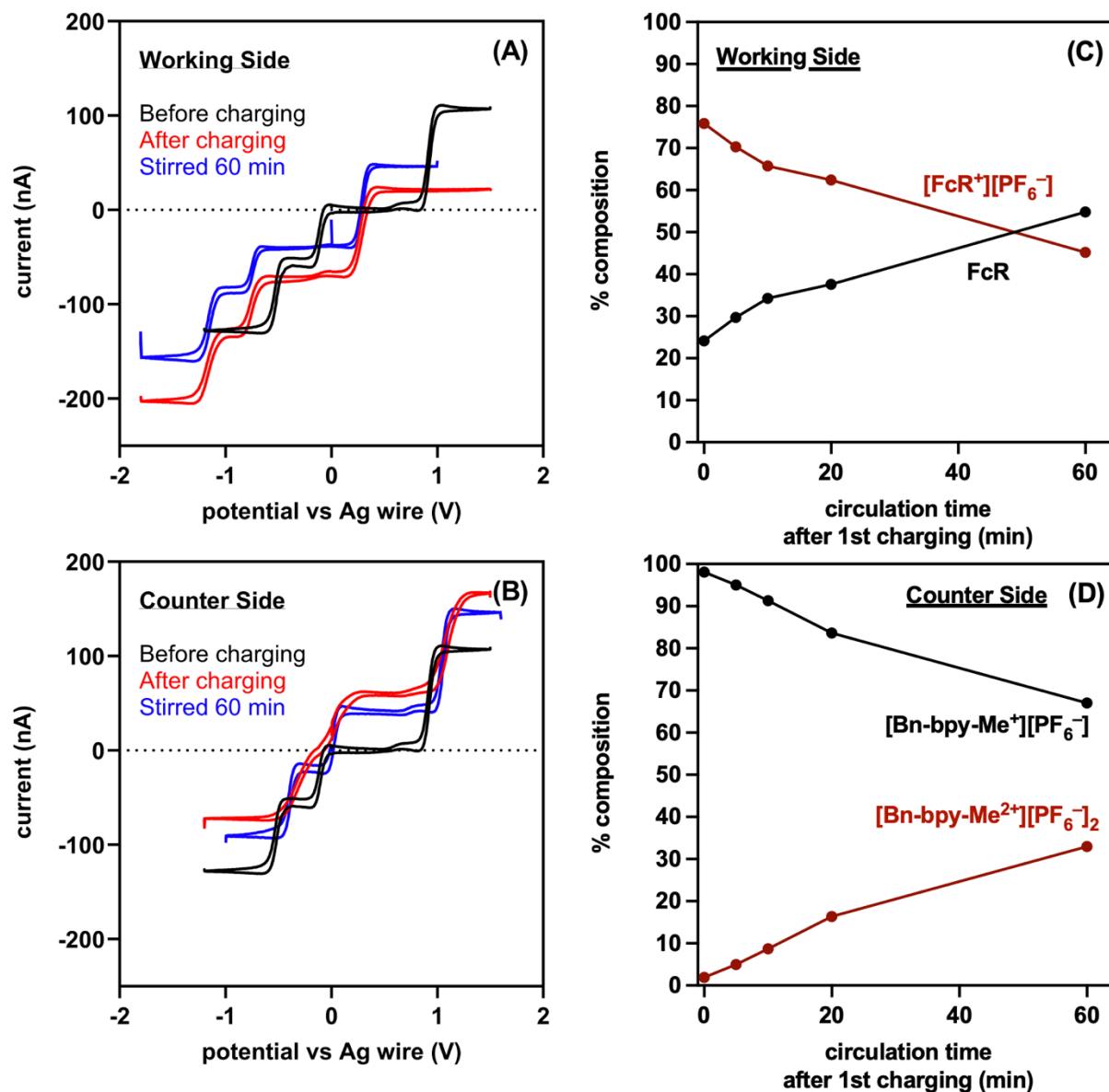


Figure S11. (A) Ultramicroelectrode cyclic voltammetry of working side before charging (black), after charging (red), and stirred for 60 min after charging monitored by a microelectrode with 2 sheets of Celgard membrane. (B) Cyclic voltammetry of counter side for the same experiment. (C) Calculated percentages of FcR and $[\text{FcR}^+][\text{PF}_6^-]$ over circulation time after charging. (D) Calculated percentages of $[\text{Bn-bpy-Me}^{2+}][\text{PF}_6^-]_2$ and $[\text{Bn-bpy-Me}^+][\text{PF}_6^-]$ over circulation time after charging.

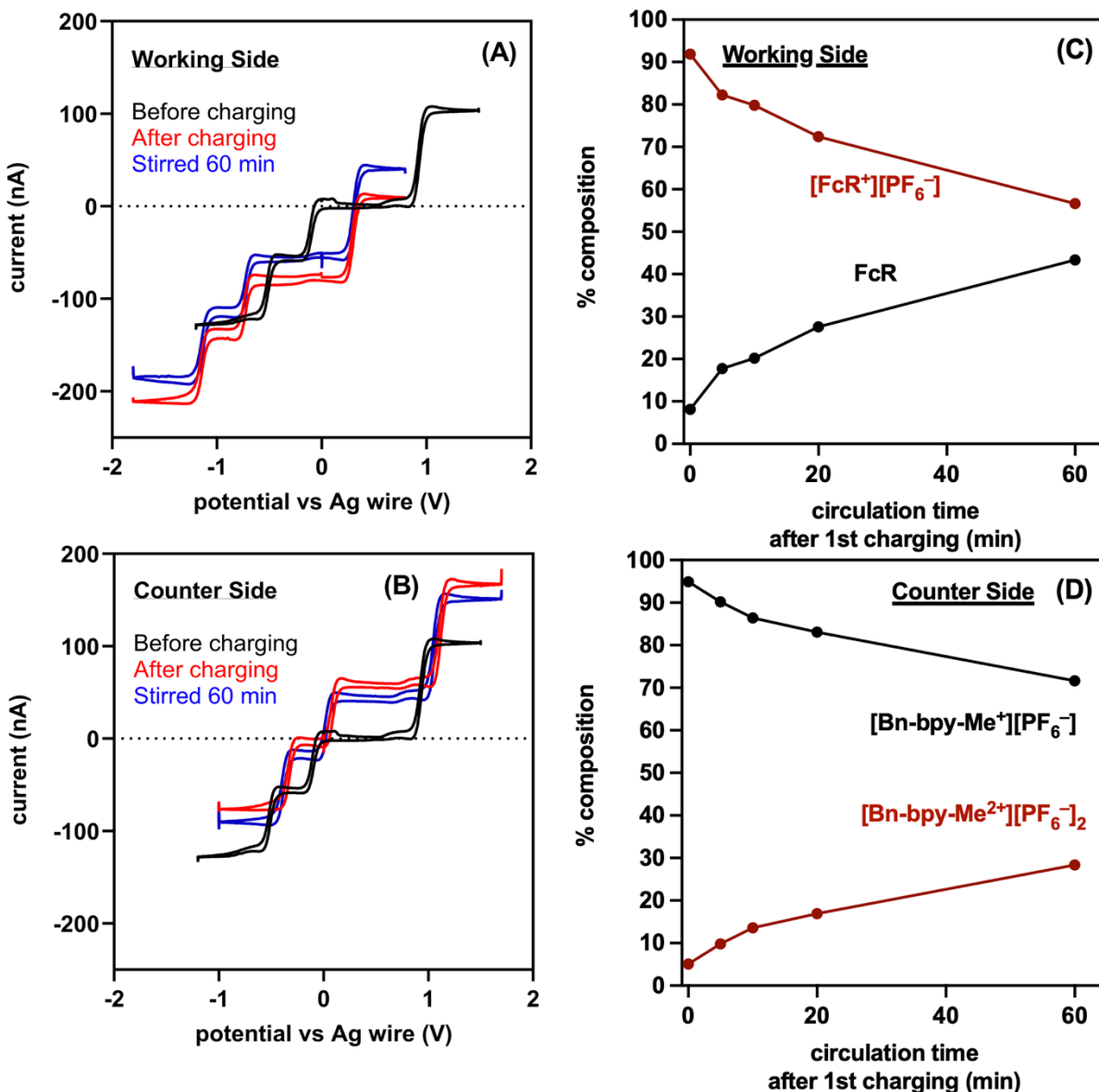


Figure S12. (A) Ultramicroelectrode cyclic voltammetry of working side before charging (black), after charging (red), and stirred for 60 min after charging monitored by a microelectrode with 1 sheet of Daramic membrane. (B) Cyclic voltammetry of counter side for the same experiment. (C) Calculated percentages of FcR and $[\text{FcR}^+][\text{PF}_6^-]$ over circulation time after charging. (D) Calculated percentages of $[\text{Bn-bpy-Me}^{2+}][\text{PF}_6^-]_2$ and $[\text{Bn-bpy-Me}^+][\text{PF}_6^-]$ over circulation time after charging.

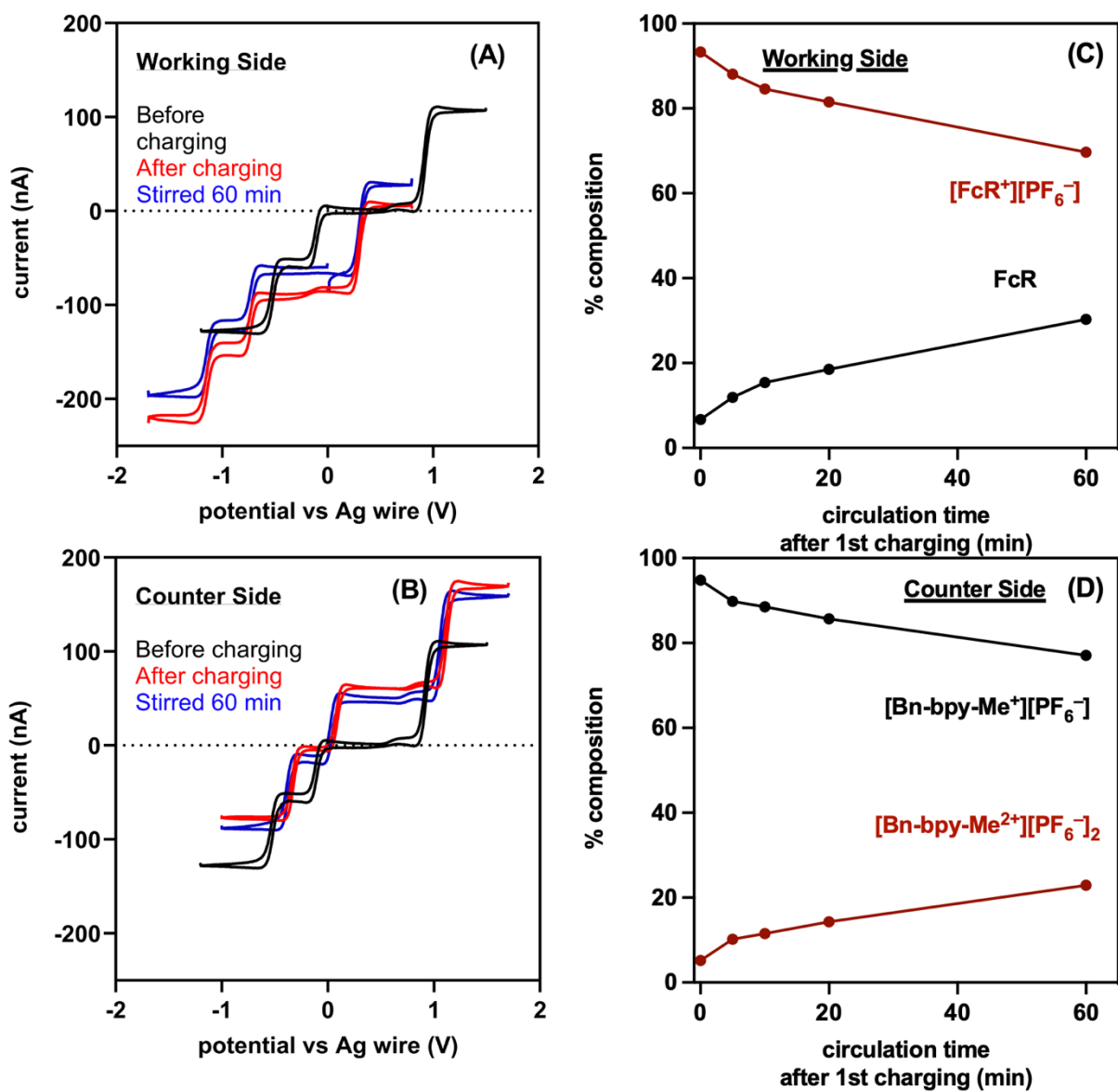


Figure S13. (A) Ultramicroelectrode cyclic voltammetry of working side before charging (black), after charging (red), and stirred for 60 min after charging monitored by a microelectrode with **2 sheets of Daramic membrane**. (B) Cyclic voltammetry of counter side for the same experiment. (C) Calculated percentages of **FcR** and $[FcR^+][PF_6^-]$ over circulation time after charging. (D) Calculated percentages of $[Bn-bpy-Me^{2+}][PF_6^-]_2$ and $[Bn-bpy-Me^+][PF_6^-]$ over circulation time after charging.

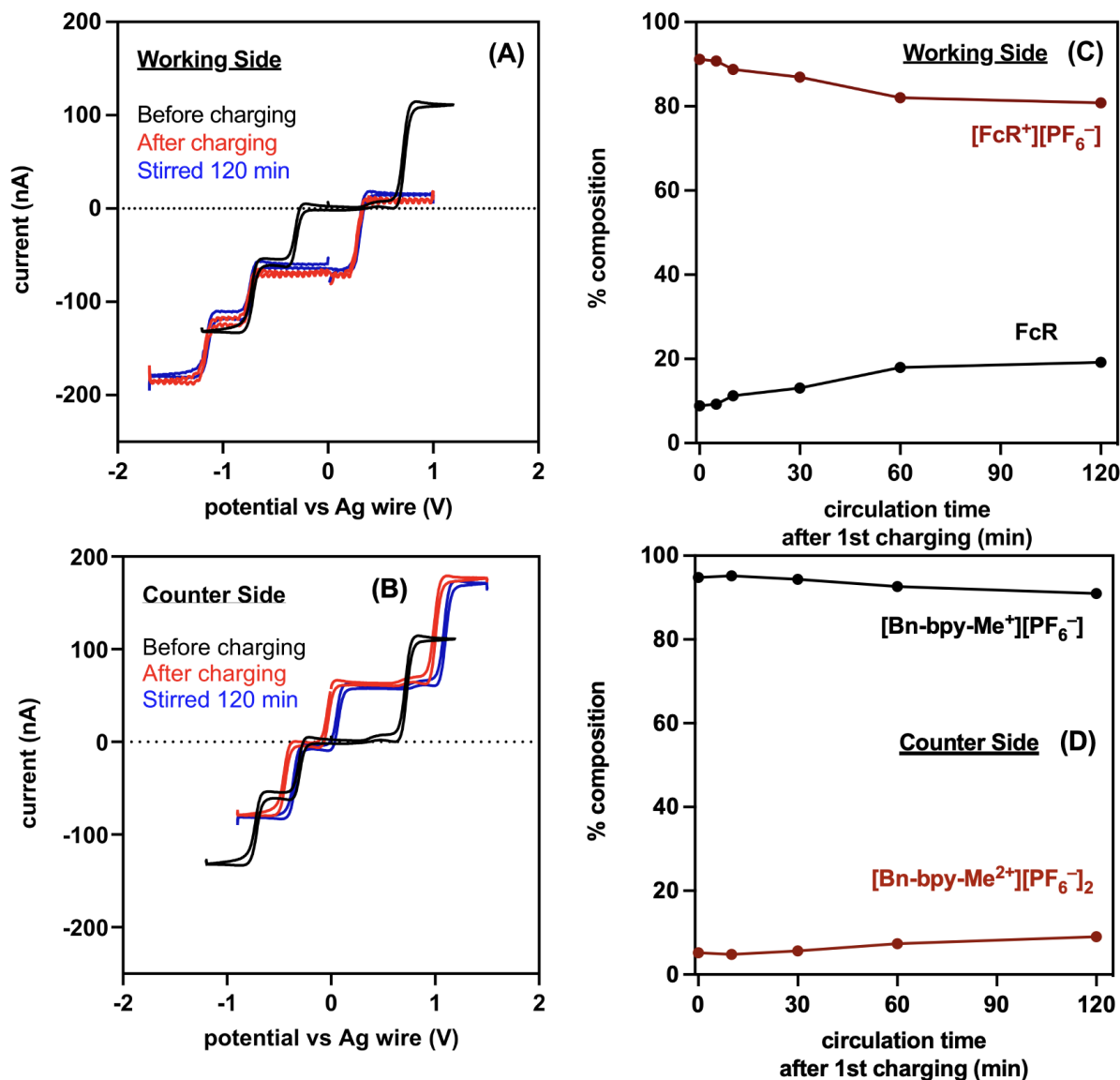


Figure S14. (A) Ultramicroelectrode cyclic voltammetry of working side before charging (black), after charging (red), and stirred for 60 min after charging monitored by a microelectrode with 1 sheet of Fumasep membrane. (B) Cyclic voltammetry of counter side for the same experiment. (C) Calculated percentages of FcR and $[\text{FcR}^+][\text{PF}_6^-]$ over circulation time after charging. (D) Calculated percentages of $[\text{Bn-bpy-Me}^{2+}][\text{PF}_6^-]_2$ and $[\text{Bn-bpy-Me}^+][\text{PF}_6^-]$ over circulation time after charging.

XIII. Flow Cell Cycling with Celgard Membrane or with xPS-CI Beads

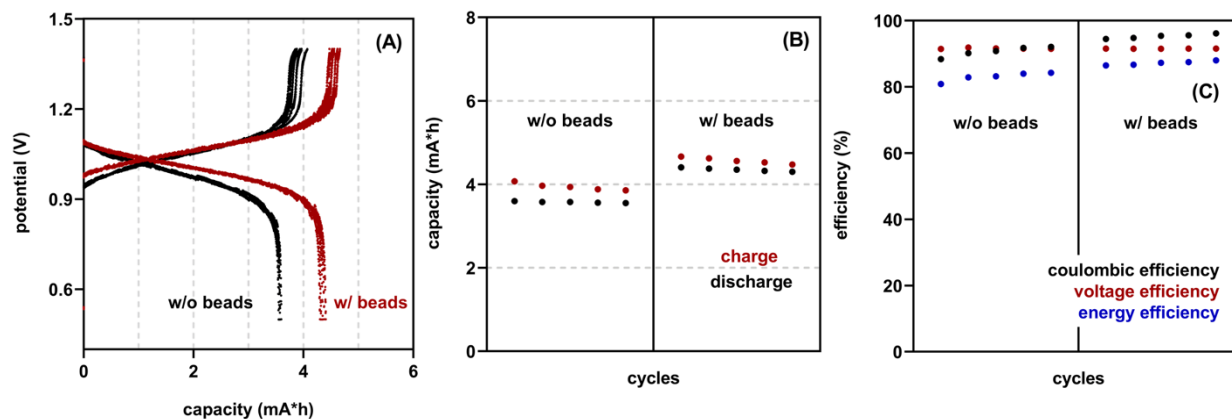


Figure S15. RMFB data with or without 1 equiv. functionalized beads using 2 sheets of Celgard membrane. Plots of (A) potential versus capacity, (B) capacity versus cycles, and (C) efficiency versus cycles.

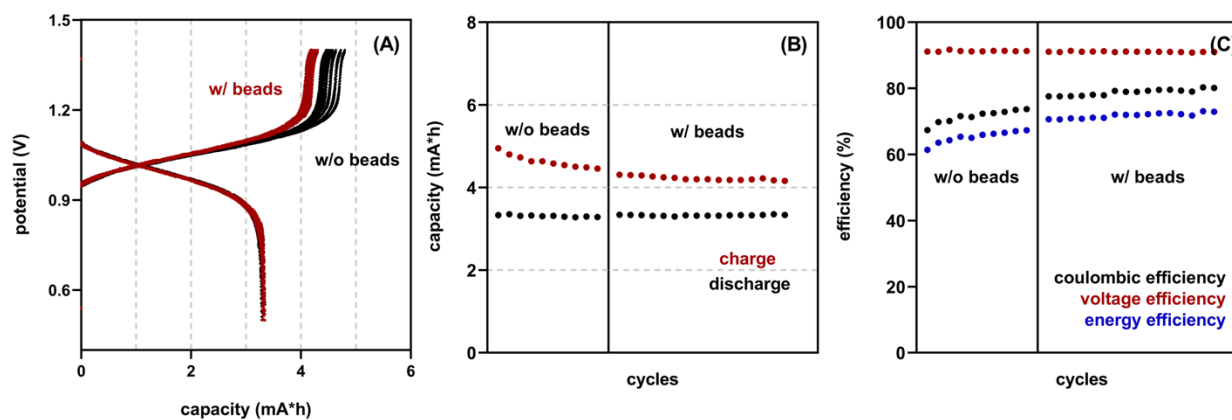


Figure S16. RFB data with or without 1 equiv. xPS-CI (unfunctionalized beads) with 2 sheets of Celgard membrane. Plots of (A) potential versus capacity, (B) capacity versus cycles, and (C) efficiency versus cycles. Data indicated that unfunctionalized beads had no impact on RFB.

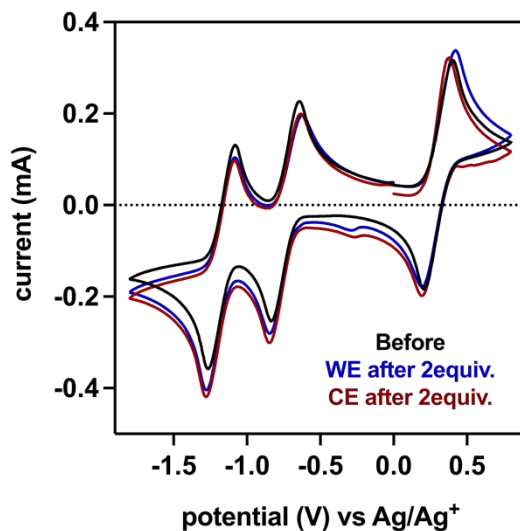


Figure S17. Post-run cyclic voltammetry of electrolyte solutions of RMFB (with 2 equiv of beads) before and after cycling. Black CV is before cycling, blue CV (“WE”) is catholyte after cycling, red CV (“CE”) is anolyte after cycling.

XIV. References

¹ Xiao, Y.; Chu, L.; Sanakis, Y.; Liu, P. Revisiting the IspH catalytic system in the deoxyxylulose phosphate pathway: achieving high activity. *J. Am. Chem. Soc.* **2009**, *131*, 9931–9933.

² Nchimi-Nono, K.; Dalvand, P.; Wadhwa, K.; Nuryyeva, S.; Alneyadi, S.; Prakasam, T.; Trabolsi, A. Radical-Cation Dimerization Overwhelms Inclusion in [n] Pseudorotaxanes. *Chem. Eur. J.* **2014**, *20*, 7334–7344.

³ Milshtein, J. D.; Kaur, A. P.; Casselman, M. D.; Kowalski, J. A.; Modekrutti, S.; Zhang, P. L.; Attanayake, N. H.; Elliott, C. F.; Parkin, S. R.; Risko, C.; Brushett, F. R.; Odom, S. A. High Current Density, Long Duration Cycling of Soluble Organic Active Species for Non-Aqueous Redox Flow Batteries. *Energy Environ. Sci.* **2016**, *9*, 3531–3543.